Random Potential Effect near the Bicritical Region in Perovskite Manganites as Revealed by Comparison with the Ordered Perovskite Analogs

D. Akahoshi,[1] M. Uchida,[2] Y. Tomioka,[1] T. Arima,[3,4] Y. Matsui,[2] and Y. Tokura[1,4,5]

[1]*Correlated Electron Research Center (CERC), Advanced Industrial Science and Technology (AIST), Tsukuba 305-8562, Japan*
[2]*Advanced Materials Laboratory, National Institute for Materials Science, Tsukuba, 305-0044, Japan*
[3]*Institute of Materials Science, University of Tsukuba, Tsukuba 305-8573, Japan*
[4]*Spin Superstructure Project, ERATO, JST, C/O AIST, Tsukuba 305-8562, Japan*
[5]*Department of Applied Physics, University of Tokyo, Tokyo 113-8656, Japan*

(Received 3 September 2002; published 2 May 2003)

The orbital-charge-spin ordering phase diagram for half-doped perovskites $Ln_{1/2}Ba_{1/2}MnO_3$ (Ln = rare earth) with ordered Ln/Ba cations has been investigated comparatively with that of the Ln/Ba solid-solution analogs. A large modification of the phase diagram is observed upon the *A*-site disordering near the original bicritical point between the charge-orbital ordering and ferromagnetic metallic phases. The random potential by quenched disorder inherent in the *A*-site solid solution is found to suppress the respective long-range orders and gives rise to the colossal magnetoresistive state.

DOI: 10.1103/PhysRevLett.90.177203 PACS numbers: 71.30.+h, 75.30.Kz

The perovskite manganites have been attracting much interest because of their rich and intriguing magnetic and electronic properties [1,2]. Recent studies have revealed the close interplay among spin, charge, orbital, and lattice degrees of freedom as the source of complex behaviors in the manganites. Competing interactions/orders inherent in the manganites, such as between double-exchange ferromagnetism and superexchange antiferromagnetism and/or between charge/orbital order and metallic state, tend to produce the bicritical state where external stimuli occasionally cause the phase transformation, e.g., between a metal and an insulator, and/or between a ferromagnet and an antiferromagnet. The colossal magnetoresistance (CMR) phenomena are one such example. The disorder in such a critical region of the manganites may produce the phase separation in the competing two ordered phases on various time scales and length scales [3–6]. The most typical example is the relaxor-like effect induced by Cr doping on the Mn sites in the charge/orbital ordered (CO/OO) state, which gives rise to the ferromagnetic (FM) metallic clusters coexisting with the background CO/OO state [7–9].

Such an effect of the random potential arising from the chemical disorder is seen not only in the case of the impurity doping on the Mn sites but also in the conventional random alloying on the perovskite *A* site with rare-earth (Ln^{3+}) and alkaline-earth (Ae^{2+}) ions. The latter effect is sometimes argued in terms of the difference (standard deviation) in the ionic radii of the Ln^{3+} and Ae^{2+} cations [10–12]. Here, we show an example of the least chemical disorder attained in the sheetlike Ln-Ae ordered perovskite manganites, which can in turn visualize more clearly the dramatic effect of the quenched disorder inherent to the Ln-Ae solid solution in the bicritical region.

The half-doped manganites $Ln_{1/2}Ba_{1/2}MnO_3$ may give a good arena to test the above idea. The perovskite manganites in this chemical composition have two possible forms of the crystal structure [see Figs. 1(a) and 1(b)] depending on the synthetic condition [13]. One is the *A*-site disordered (solid-solution) structure [Fig. 1(b)], and the other is the *A*-site ordered perovskite with the alternate stack of LnO and BaO sheets along the *c* axis with intervening MnO_2 sheets [Fig. 1(a)]. Millange *et al.* first studied the difference between the *A*-site ordered and disordered perovskites in the case of Ln = La and reported that the ground states of both materials are the FM metal with different Curie temperatures (T_C) [13]. Ueda *et al.* reported that the charge-ordering (CO) transition temperature (T_{CO}) can be as high as 500 K for the ordered form of $Y_{1/2}Ba_{1/2}MnO_3$ [14] as opposed to the T_{CO} of 200–250 K in the conventional *A*-site solid-solution $Ln_{1/2}Ca_{1/2}MnO_3$ [1,2].

The *A*-site ordered form of $Ln_{1/2}Ba_{1/2}MnO_3$ (Ln = La–Tb) was prepared by solid state reaction in a polycrystalline form. Mixed powders of Ln_2O_3 (except for Pr_6O_{11} and Tb_4O_7), $BaCO_3$, and Mn_3O_4 were treated in Ar atmosphere at 1623–1773 K with a few intermediate grindings and then annealed at 973 K in O_2 atmosphere. The *A*-site solid solutions of $Ln_{1/2}Ba_{1/2}MnO_3$ (Ln = La–Dy) were grown by the floating-zone method in a single-crystalline form. The magnetic properties were measured with a SQUID magnetometer, and the transport properties were measured with a four-probe method. Transmission electron microscopy (TEM) experiments were performed with an Hitachi HF-3000S operating at 300 kV.

The *A*-site ordering and disordering can be clearly discerned in the lattice image [Figs. 1(c) and 1(d)] obtained by high resolution transmission electron microscopy (HRTEM), e.g., for the Ln = Sm case. Modulation of the distance between adjacent MnO_2 layers is seen in the HRTEM image of the ordered material, attributed to the *A*-site ordering of Sm and Ba ions. No modulation is

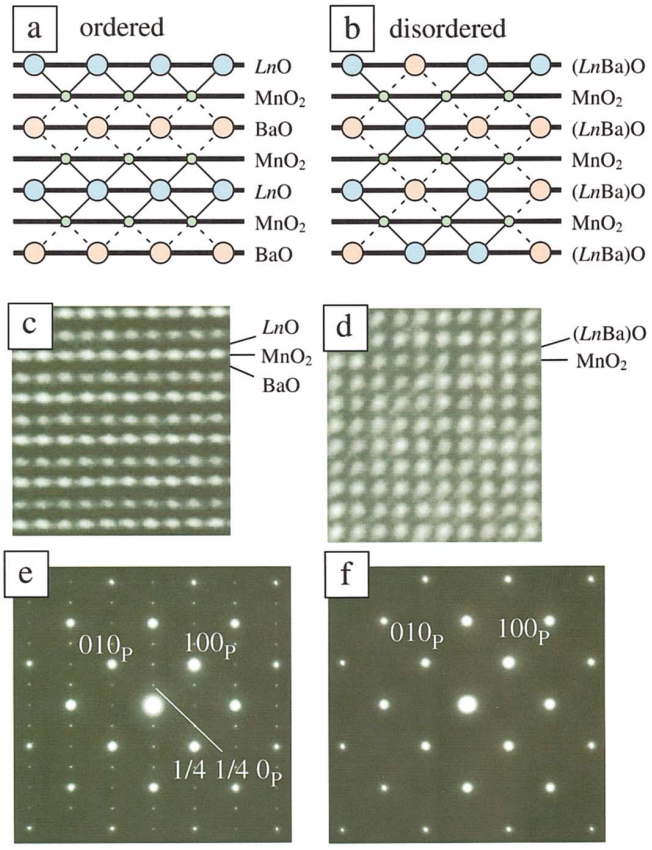

FIG. 1 (color). Schematic structures of half-doped perovskite, $Ln_{1/2}Ba_{1/2}MnO_3$, viewed along the b axis: (a) the A-site ordered perovskite with the alternate stack of LnO and BaO layers along the c axis, and (b) the A-site disordered (solid-solution) perovskite with cubic structure. The lattice images obtained by high resolution transmission electron microscopy (HRTEM) at room temperature are shown for (c) the A-site ordered and (d) disordered $Sm_{1/2}Ba_{1/2}MnO_3$. The [001]-zone electron-diffraction pattern of (e) the A-site ordered and (f) disordered $Sm_{1/2}Ba_{1/2}MnO_3$ at room temperature. The superlattice reflections with a modulation wave vector (1/4, 1/4, 0) are clearly observed in the ordered material, proving the presence of the charge/orbital ordered phase. These superlattice reflections disappear above 380 K. For the disordered material, no superlattice reflection is observed down to low temperature, indicating no long-range charge/orbital order.

observed in the HRTEM image of the A-site disordered material. This A-site ordering is due to the large difference in the ionic radii of Ln^{3+} and Ba^{2+} and reminiscent of the structure of well-known 123-type high-temperature superconductors, $LnBa_2Cu_3O_7$. The respective MnO_2 sheets in this A-site ordered tetragonal form are free from random potential which would otherwise arise from the Coulomb potential and/or local strain via the random Ln^{3+}/Ba^{2+} A sites. By contrast, the melt-grown sample with the same A-site composition shows the complete solid solution of Ln and Ba ions on the A sites with a simple cubic form as the average structure.

We show in Fig. 2 the electronic phase diagrams both for the A-site ordered and disordered forms of $Ln_{1/2}Ba_{1/2}MnO_3$ with a variation of Ln. On the basis of the appreciable modification of the electronic phase diagram upon the A-site disordering, we argue the important effect of A-site disorder near the bicritical region of the manganites.

Let us begin with the comparison between the A-site ordered and disordered forms of $Sm_{1/2}Ba_{1/2}MnO_3$. The temperature (T) dependence of the magnetization and electrical resistivity are shown in Fig. 3. In the ordered form [Fig. 3(a)], the magnetization and resistivity simultaneously exhibit abrupt changes at 380 K where the structure changes from tetragonal with the lattice parameters of $a = 3.915$ Å and $c = 7.622$ Å at 300 K to orthorhombic with those of $a = 3.914$ Å, $b = 3.882$ Å, and $c = 7.692$ Å at 380 K. The lattice-structural change is clearly ascribed to the onset of the charge/orbital order [14–17]. Figure 1(e) shows the electron diffraction projected on the [001] zone in the tetragonal setting, in which distinct superlattice spots (1/4, 1/4, 0) arising from the diagonal orbital/charge stripes on the Mn square lattice are discerned. The suggested orbital/charge ordering pattern [15,16] is identical in the ab plane with that of the conventional disordered manganites [18,19], but differs in its stacking pattern ($AABB$ type) along the c axis. Recent results of resonant x-ray diffraction and its azimuthal angle dependence [20] also support this assignment. Other A-site ordered materials with the ionic radius of Ln smaller than that of Sm have the same CO/OO pattern as $Sm_{1/2}Ba_{1/2}MnO_3$, and T_{CO} is raised with the decrease

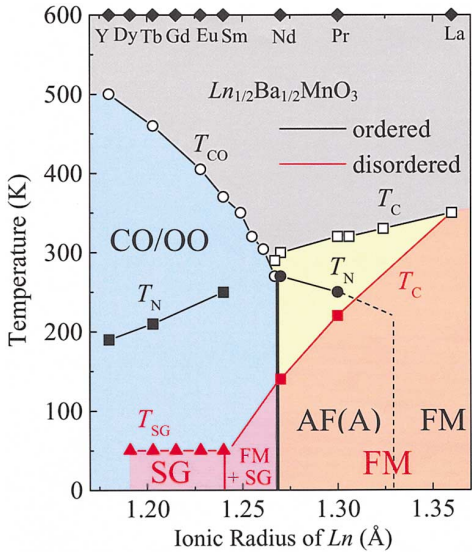

FIG. 2 (color). Electronic phase diagrams for the A-site ordered (black line and symbols) and disordered (red line and symbols; the region shaded in red) perovskites with half doping $Ln_{1/2}Ba_{1/2}MnO_3$, as a function of the ionic radius of Ln. CO/OO, FM, and SG stand for the charge/orbital ordered, ferromagnetic, and spin-glass states, respectively. T_{CO}, T_C, and T_{SG} represent the respective transition temperatures. The data for the mixed crystal compounds with Ln = (Nd, Sm) and (La, Nd), both Ln/Ba ordered and disordered, are also shown.

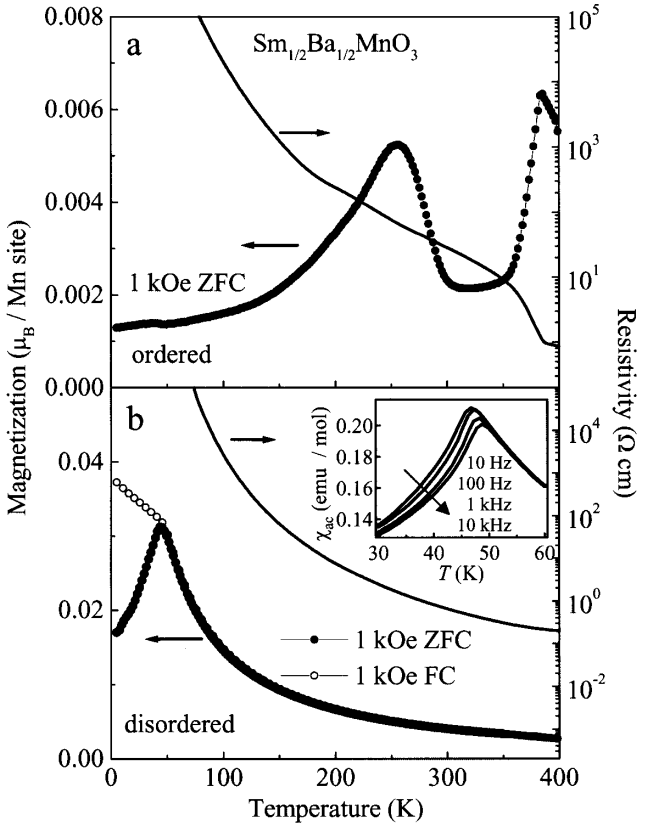

FIG. 3. Temperature dependence of magnetization and resistivity for (a) the *A*-site ordered and (b) disordered $Sm_{1/2}Ba_{1/2}MnO_3$. The inset of (b) indicates the frequency dependence of the ac susceptibility (χ_{ac}). ZFC and FC represent the zero-field-cooling and field-cooling processes, respectively. No significant difference is observed between ZFC and FC measurements in the ordered system. The magnetization and resistivity of the ordered material shows an abrupt change at around 380 K, above which the superlattice reflections [Fig. 1(e)] disappear.

of ionic radius of Ln, as shown in Fig. 2. The magnetization peak around 250 K ($= T_N$) corresponds to the antiferromagnetic transition [16].

On the other hand, the resistivity of the *A*-site disordered $Sm_{1/2}Ba_{1/2}MnO_3$ shows no distinct anomaly, and the magnetization behavior, such as a difference in field cooling and zero-field cooling [Fig. 3(b)] and the frequency dependence of the ac susceptibility [the inset to Fig. 3(b)], indicate the presence of the spin-glass-like state below 50 K. In accord with this, no superlattice diffraction spot is discerned by the TEM observation [Fig. 1(f)]. These results suggest that the random potential originating in the *A*-site disorder totally suppresses the long-range order in the charge and orbital sectors to give rise to the spin-glass state at a lower temperature. The glass state appears below 50 K also in other *A*-site disordered compounds with Ln = Eu–Dy (Fig. 2).

The magnetic and transport properties of $Nd_{1/2}Ba_{1/2}MnO_3$ are shown in Fig. 4. In the *A*-site ordered $Nd_{1/2}Ba_{1/2}MnO_3$, the magnetic transitions can be seen around 300 and 270 K. The steep onset of the magnetization around 300 K may indicate the onset of the FM state or the strong FM fluctuation. Around 270 K, the magnetization and resistivity simultaneously show a steep change. Powder neutron diffraction experiments [21] proved that the magnetization anomaly at 270 K is due to the onset of the *A*-type antiferromagnetic (AFM) state. The *ab* plane is FM associated with the ordering of $d_{x^2-y^2}$ orbitals and stacks antiferromagnetically along the *c* axis. The *A*-type AFM phase adjacent to the FM state is well known for the nearly half-doped manganites [22]. To seek for the origin of the abrupt phase change between the Ln = Sm (Fig. 3) and Ln = Nd (Fig. 4) compound, we further investigated the physical properties of the Ln/Ba-site ordered and the Ln-site mixed-crystal system $(Sm_{1-y}Nd_y)_{1/2}Ba_{1/2}MnO_3$. We found that in the clean limit the two ordered states, i.e., the CO/OO and FM states, appear to meet at around Ln = Nd ($y = 1$). Thus, the ordered $Nd_{1/2}Ba_{1/2}MnO_3$ is close to the multicritical point where the three ordered states, i.e., FM, *A*-type AFM, and CO/OO states, compete with each other. T_C

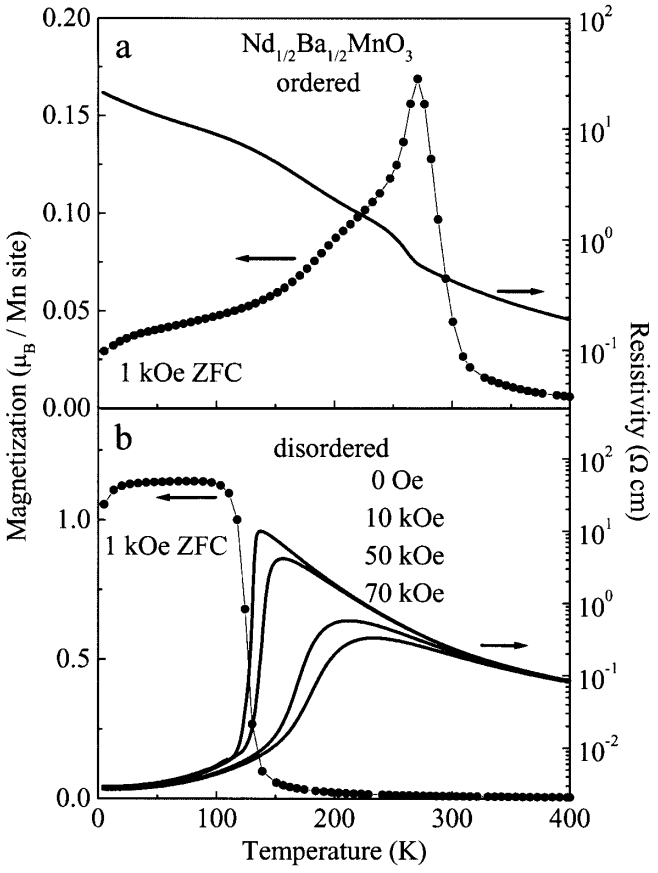

FIG. 4. Temperature dependence of magnetization and resistivity for (a) the *A*-site ordered and (b) disordered $Nd_{1/2}Ba_{1/2}MnO_3$. No significant difference is seen between ZFC and FC measurements in both systems. The *A*-site disordered material shows the typical CMR behavior around T_C. Note the logarithmic scale on the ordinate for the resistivity.

of the ordered $Ln_{1/2}Ba_{1/2}MnO_3$ shows an increase with the change of the Ln ion from Nd (300 K) to La (350 K) as seen in Fig. 2, while the *A*-type AFM phase extinguishes between Ln = Pr and La. In contrast, the *A*-site disorder in $Nd_{1/2}Ba_{1/2}MnO_3$ locating near the original bicritical (multicritical) point tends to suppress such a long-range order. The magnetic and electrical properties of the disordered $Nd_{1/2}Ba_{1/2}MnO_3$ as observed in Fig. 4(b) indicate that the ground state is the FM metal with much decreased T_C of 140 K and that a typical CMR effect accompanying the resistivity change by 3 orders of magnitude is observed near above T_C.

In Fig. 2, we have summarized the present results as the electronic phase diagram for $Ln_{1/2}Ba_{1/2}MnO_3$ for both the *A*-site order (black line and symbols) and disorder (red line and symbols). The T_{CO} is as high as 500 K for the ordered form of $Y_{1/2}Ba_{1/2}MnO_3$ as the smallest-Ln compound [14], but it steeply decreases with increasing the Ln ionic size. On the other hand, the T_C decreases with decreasing the Ln ionic size. Finally, both transition temperatures for the competing phases meet to coincide at around Ln = Nd, forming the bicritical point. As seen in Fig. 1(a), the MnO_2 sheets sandwiched by the ordered LnO and BaO layers suffer from no random potential. By contrast, the *A*-site disorder as illustrated in Fig. 1(b) generates the random Coulomb potential between the MnO_2 sheets and the (LnBa)O layers as well as the random local lattice distortion. For the Mn^{3+}/Mn^{4+}-alternate CO state, this should cause the frustration effect as well. In fact, the randomness of the solid-solution *A*-site was found to result in a large modification in the electronic phase diagram of $Ln_{1/2}Ba_{1/2}MnO_3$, as indicated in Fig. 2. First, the long-range order in the charge and orbital sectors with a relatively high transition temperature T_{CO} totally collapses in this *A*-site disordered system and remains dynamical down to the spin-glass transition temperature of about 50 K, as shown in Fig. 3(b).

The disorder on the perovskite *A* site appears to produce a further unique feature near the original bicritical (or multicritical) point. The T_C tends to be critically suppressed with decreasing the Ln ionic radius as compared with the *A*-site ordered case. For Ln = Nd, which would locate near the bicritical point in the ordered form, T_C is most reduced by the *A*-site alloying. The charge-orbital correlation as evidenced by x-ray diffuse scattering tends to grow with lowering temperature in this compound, but suddenly disappears at T_C, as generally observed for the CMR manganites [1], in accord with the sharp and gigantic drop of resistivity at T_C [Fig. 4(b)]. It is well known that the CMR effect is maximized in such a most reduced-T_C material as the present *A*-site disordered $Nd_{1/2}Ba_{1/2}MnO_3$. The modification of the electronic phase diagram as induced by the *A*-site disorder is partly in accord with the theoretical prediction based on a simplified model by Burgy *et al.* [23]. According to their model, the classical bicritical feature arising from the competition between the CO and FM states is modified to such that the respective transition temperatures are suppressed to form the microscopically phase-separated region near the original bicritical point and to give rise to a quantum critical-like feature. The sharp decrease of T_C with decreasing ionic radius of Ln as observed only in the *A*-site disordered case may correspond to such a situation.

In conclusion, we have comparatively investigated the electronic properties and phase diagrams for the perovskite manganites with and without the intrinsic structural disorder. We have revealed that the *A*-site disorder not only produces the glassy state but also enhances the fluctuation of the competing orders, i.e., between the charge/orbital order and the metallic ferromagnetism, near the original bicritical point. Such a large fluctuation as induced by *A*-site disorder, that is amenable to an external magnetic field favoring the metallic FM phase, is one of the most essential ingredients of the CMR physics.

We thank N. Nagaosa and H. Takagi for helpful discussions. This work was supported in part by NEDO.

[1] Y. Tokura and N. Nagaosa, Science **288**, 462 (2000).
[2] E. Dagotto, T. Hotta, and A. Moreo, Phys. Rep. **344**, 1 (2001).
[3] S. Mori, C. H. Chen, and S-W. Cheong, Phys. Rev. Lett. **81**, 3972 (1998).
[4] Y. Moritomo, Phys. Rev. B **60**, 10 374 (1999).
[5] A. Moreo, S. Yunoki, and E. Dagotto, Science **283**, 2034 (2000).
[6] M. Uehara *et al.*, Nature (London) **399**, 560 (1999).
[7] A. Barnabe *et al.*, Appl. Phys. Lett. **71**, 3907 (1997).
[8] B. Raveau, A. Maignan, and C. Martin, J. Solid State Chem. **130**, 162 (1997).
[9] T. Kimura *et al.*, Phys. Rev. Lett. **83**, 3940 (1999).
[10] J. P. Attfield *et al.*, Chem. Mater. **10**, 3239 (1998).
[11] P. W. Woodward *et al.*, Chem. Mater. **10**, 3652 (1998).
[12] L. M. Rodríguez-Martínez and J. P. Attfield, Phys. Rev. B **63**, 024424 (2000).
[13] F. Millange *et al.*, Chem. Mater. **10**, 1974 (1998).
[14] T. Nakajima, H. Kageyama, and Y. Ueda, J. Phys. Chem. Solids **63**, 913 (2002).
[15] M. Uchida *et al.*, J. Phys. Soc. Jpn. **71**, 2605 (2002).
[16] T. Arima *et al.*, Phys. Rev. B **66**, 140408 (2002). The neutron diffraction of the ordered $Tb_{1/2}Ba_{1/2}MnO_3$ indicated that the charge-orbital ordering sequence along the *c* axis changes from *AABB* to *ABAB* type below T_N. The spin ordering structure on the *ab* plane is similar to the conventional CE type, but its structure along the *c* axis is an up-up-down-down type.
[17] T. Nakajima *et al.*, J. Phys. Soc. Jpn. **71**, 2843 (2002).
[18] E. O. Wollan and W. C. Koehler, Phys. Rev. **100**, 545 (1955).
[19] B. J. Sternlieb *et al.*, Phys. Rev. Lett. **76**, 2169 (1996).
[20] D. Akahoshi *et al.* (unpublished).
[21] T. Arima *et al.* (unpublished).
[22] H. Kawano *et al.*, Phys. Rev. Lett. **78**, 4253 (1997).
[23] J. Burgy *et al.*, Phys. Rev. Lett. **87**, 277202 (2001).